

Chitosan nanoparticles for tamoxifen delivery and cytotoxicity to MCF-7 and Vero cells*

Neralakere Ramanna Ravikumara^{1,2} and Basavaraj Madhusudhan^{2,‡}

¹Department of Biochemistry, P.G. Centre, Kuvempu University, Shivagangothri, Davanagere 577 002, Karnataka, India; ²Research Center for Nanoscience and Technology, Department of Biochemistry and Food Technology, Davanagere University, Shivagangothri, Davanagere 577 002, Karnataka, India

Abstract: In this study, tamoxifen citrate-loaded chitosan nanoparticles (tamoxcL-ChtNPs) and tamoxifen citrate-free chitosan nanoparticles (tamoxcF-ChtNPs) were prepared by an ionic gelation (IG) method. The physicochemical properties of the nanoparticles were analyzed for particle size, zeta (ζ) potential, and other characteristics using photon correlation spectroscopy (PCS), zeta phase analysis light scattering (PALS), scanning electron microscopy (SEM), Fourier transform infrared (FTIR), and differential scanning calorimetry (DSC). The variation in particle size was assessed by changing the concentration of chitosan, pentasodium tripolyphosphate (TPP), and the pH of the solution. The optimized tamoxcL-ChtNPs showed mean diameter of 187 nm, polydispersity of 0.125, and ζ -potential of +19.1 mV. The encapsulation efficiency (EE) of tamoxifen citrate (tamoxc) increased at higher concentrations, and release of tamoxc from the chitosan matrix displayed controlled biphasic behavior. Those tamoxcL-ChtNPs tested for chemosensitivity showed dose- and time-dependent antiproliferative activity of tamoxc. Further, tamoxcL-ChtNPs were found to be hemocompatible with human red blood cells (RBCs) and safe by in vitro cytotoxicity tests, suggesting that they offer promise as drug delivery systems in therapy.

Keywords: chitosan; controlled release; encapsulation efficiency; ionic gelation; tamoxifen citrate; tripolyphosphate.

INTRODUCTION

Today, tamoxifen citrate (tamoxc) is the drug of choice for estrogen-mediated treatment among breast cancer patients [1]. The anti-estrogenic (breast) or estrogenic (uterus) activity of tamoxifen is known to be dependent on the level of dose and location of tissue. Both agonistic and antagonistic properties of tamoxifen are being exploited in the treatment of breast cancer and other related diseases [2–6]. According to de Lima and co-workers, the use of tamoxifen at low dose (0.1 μ M) generates oxidative stress and induces either cell proliferation or apoptosis in a dose-dependent manner. Unfortunately, it has been documented that dose-dependent tamoxifen therapy would induce liver cancer, increased blood clotting, retinopathy, and corneal opacities [7]. From reports, it is clear that repeated treatment would produce an acquired tamoxifen resistance followed by tumor progression [1]. In recent years, site-directed drug delivery has become a useful tool in the pharmaceutical area offering a wide range of

*Paper based on a presentation made at the International Conference on Nanomaterials and Nanotechnology (NANO-2010), Tiruchengode, India, 13–16 December 2010. Other presentations are published in this issue, pp. 1971–2113.

‡Corresponding author

actual and perceived advantages to some of the chronic diseases. In order to overcome certain undesirable side-effects, biodegradable polymers of colloidal range are being developed to deliver drugs in negligibly smaller doses to the target of interest [8,9]. Polymeric nanoparticles have been found to be good vehicles for the delivery of hydrophobic and hydrophilic drugs because they avoid possible degradation by enzymes [9,10]. In addition, high-quality chitosan from natural sources is being preferred to develop nanoparticles owing to its exceptional biodegradability, biocompatibility, and nontoxicity. Of several methods used, an ionic gelation (IG) method developed by Calvo and co-workers has been found to be the suitable system to prepare stable and biocompatible chitosan nanoparticles (ChtNPs) [11–14]. In the present study, we have attempted to prepare biodegradable tamoxc-loaded chitosan nanoparticles (tamoxcL-ChtNPs) and tamoxc-free chitosan nanoparticles (tamoxcF-ChtNPs) by an IG technique. Such nanoparticles can be characterized for physicochemical properties and evaluated for their hemocompatibility and cytotoxicity studies against both MCF-7 and Vero cells [15–18].

MATERIALS AND METHODS

Materials

Chitosan (MW of 30 kDa) was a gift sample from Laxmish I P, Cochin Central Marine Fisheries Research Institute, Cochin, India. Tamoxc was a kind gift from Arex Laboratories, Mumbai. Pentasodium tripolyphosphate (TPP) was purchased from Sigma (St. Louis, MO, USA), and acetic acid was purchased from Hi-media Chemical Co. (Mumbai, India). Double distilled water was used throughout the study. All other reagents were of analytical grade unless otherwise stated.

Determination of degree of deacetylation (DD)

The content of the acetyl group in the chitosan samples was determined by titrimetric method [19]. A standard acid–base titration was performed using phenolphthalein as an indicator. A 1 % chitosan solution (in acetic acid) added to phosphoric acid (1:1, v/v) was titrated against 0.1 M NaOH using phenolphthalein as an indicator. The DD of the chitosan sample can be obtained using the following formula:

$$DD(\%) = 100 - 2.03 \frac{V_{ch} - V_o}{m}$$

where m = amount of chitosan (mg) used and V = difference of the 0.1 M NaOH used between the chitosan solution and standard.

Preparation of tamoxc-loaded chitosan nanoparticles

ChtNPs were produced based on an IG of TPP and chitosan, as described elsewhere [20]. Nanoparticles were spontaneously obtained upon mixing the aqueous 0.08 % (w/v) TPP solution (1.2 ml) with acidic 0.2 % (w/v) chitosan solution (3 ml) using a magnetic stirrer at room temperature. TamoxcL-ChtNPs were formed by the addition of tamoxifen dissolved in methanol (5 mg/ml) to chitosan solution and followed by the TPP solution in a dropwise manner. TamoxcL-ChtNPs formed were concentrated by centrifugation (Beckman T 20 rotor, USA) at 16 000 g in a 10 μ l glycerol bed for 30 min. The supernatants were discarded, and resultant nanoparticles resuspended in water with sucrose (5 %) and lyophilized (Labconco, Kansas City, MO, USA). In order to examine the effect of concentration of reacting molecules on particle size and encapsulation efficiency (EE), a range of chitosan (0.100, 0.120, 0.144, 0.160, 0.200, 0.250, and 0.300 % (w/v)) and TPP (0.020, 0.040, 0.060, 0.080 and 0.100 % (w/v)) were used. TamoxcF-ChtNPs were prepared in the same way by omitting the drug tamoxifen.

Physical characterization of ChtNPs

Morphology of ChtNPs

Scanning electron microscopy (SEM) was performed using a LEO 1530 (LEO Electron Microscopy Inc., Thornwood, NY) operating between 15 and 20 kV with a magnification of 10 to 15 K and scan speed of 10 to 12. The samples were deposited on carbon stubs, dried at room temperature, and coated with a gold layer using a Cressington sputter-coater with a rotary planetary-tilt stage, along with a thickness controller.

Particle size distribution

The nanoparticle size was determined by photon correlation spectroscopy (PCS) (Zetasizer 4000, Malvern Instruments Ltd., Malvern, UK). It's a routine method to determine the mean hydrodynamic diameter and the particle size distribution (polydispersity index, $PDI = 22/\Gamma 2$) of the nanoparticles. The dynamic light-scattering measurements were done with a wavelength of 532 nm at 25 °C with an angle detection of 90°.

Determination of ζ -potential

The zeta (ζ) potential of ChtNPs was measured from the mobility of the electrons of nanoparticles using laser doppler electrophoresis (Zetasizer Nano series, Malvern Instruments Ltd., Worcestershire, UK). The measurements were carried out in a 1 mM/L solution of NaCl (pH 6.8) by adjusting suitable dilutions (1/200, v/v) of the nanoparticle suspensions.

Fourier transform infrared spectroscopy (FTIR) analysis

The FTIR spectrum of the specimen was recorded with Nicolet IR 200 (Thermo Electron Corporation, USA). FTIR spectra were taken in the wavelength region 4000 to 400 cm^{-1} at room temperature using potassium bromide pellets (Merck, IR grade) for tamoxcF-ChtNPs, tamoxcL-ChtNPs, and tamoxc. The samples were allowed to form pellets at pressure of 10.3×10^4 Pa.

Differential scanning calorimetry (DSC)

The thermal behavior of the tamoxcF-ChtNPs, tamoxcL-ChtNPs, and tamoxc was characterized by DSC (Mettler-Toledo DSC). Approximately 3 to 6 mg of the freeze-dried particles were weighed into an aluminum pan. The nanoparticles were heated from 30 to 360 °C at a heating rate of 10 °C/min per cycle. Inert atmosphere was maintained by purging nitrogen at the flow rate of 100 ml/min.

Evaluation of encapsulation efficiency (EE)

The drug content in the prepared tamoxcL-ChtNPs was calculated by the difference between the total amount of tamoxc added during the preparation and the amount of drug present in the supernatant after centrifugation. The tamoxc present in the supernatant was determined spectrophotometrically by reading the absorbance at 249 nm (UV-vis spectrophotometer Shimadzu 1650, Kyoto, Japan).

Drug release studies

Drug release studies were carried out by dialysis method. TamoxcL-ChtNPs were redispersed in pH 7.4 PBS (5 ml) and taken into dialysis membrane bag (12 kDa) after tying at both the ends. The bag was placed in PBS (150 ml) containing jar and incubated at 37 °C in a continuous shaking water bath at 50 rpm. The amount of tamoxc released was measured by sampling out 1 ml each time at predetermined time intervals (0.5, 1, 2, 3, 4, 6, 8, 10, 12, 16, 20, 24, 36, and 48 h). From an aliquot, the amount of tamoxc released was determined spectrophotometrically at 249 nm. A standard calibration curve was drawn using tamoxc as reference standard.

Blood compatibility

Whole blood was obtained from three healthy men (22–31 years old) and added with EDTA. The contents were mixed thoroughly. Red blood cells (RBCs) were collected by centrifuging whole blood at 1000 g for 20 min. The RBCs were washed thrice with a saline solution before being diluted with a buffer to prepare erythrocyte stock solutions with fixed concentrations of hemoglobin (3:1 centrifuged

erythrocytes:buffer saline solution). Hemolysis experiments were in accordance with a method used in our previous study [21]. Freeze-dried tamoxcF-ChtNPs, tamoxcL-ChtNPs, and tamoxc were redispersed and sonicated in a saline solution to give 0.2 % suspensions. 100 μ L of tamoxcF-ChtNPs, tamoxcL-ChtNPs, and tamoxc suspension with different concentrations were added to 1 ml of an erythrocyte stock solution. The mixtures were incubated for 1 h at 37 °C in water bath (ILE Instruments, Bangalore, India). After the centrifugation (4000 g for 10 min), an aliquot of the supernatant was read at 540 nm. The supernatant was dissolved in 2 ml of saline. The saline solution alone was used as a negative control (0 % lysis) and the distilled water as a positive control (100 % lysis). The amount of released hemoglobin was determined spectrophotometrically (UV 1650 PC Shimadzu) at 540 nm.

Percent hemolysis was calculated using the formula

$$\text{Hemolysis (\%)} = \frac{\text{Absorbance of the sample}}{\text{Absorbance of the positive control}} \times 100$$

In vitro cytotoxicity assay

Cytotoxicity of tamoxcL-ChtNPs against MCF-7 and Vero cells

MCF-7 cells were cultured in Dulbecco's modified Eagle's medium (DMEM) (Sigma, Dorset, UK) without phenol red and supplemented with 10 % FBS. The cell culture medium was maintained at 37 °C in a humidified incubator containing 5 % CO₂ atmosphere. Trypsinized confluent cell monolayers (75–80 %) and the cells in the exponentially growing phase were used for cytotoxicity experiments.

MTT assay for in vitro cell viability studies

The cytotoxicity tests of tamoxcL-ChtNPs and tamoxcF-ChtNPs against MCF-7 and Vero cells were assessed using MTT assay [22]. The cytotoxicity of the nanoparticles was determined after 24 h incubation with MCF-7 and Vero cells. To determine cell cytotoxicity/viability, the cells were plated at a density of 5 \times 10³ cells/well (optimal seeding density) in 96 well plates at 37 °C in 5 % CO₂ atmosphere. After 12 h of incubation, the medium in the wells was replaced with the fresh medium containing nanoparticles of varying concentrations. After 24 h, MTT dye solution (20 μ L, 5 mg/ml in phosphate buffer pH-7.4) was added to each well. The incubation was further continued for another 2 h at 37 °C and 5 % CO₂ for exponentially growing cells. Then, the medium in each well containing unbound MTT and dead cells was removed by suction. The formazan crystals were solubilized with 100 μ L of DMSO, and the solution was vigorously mixed to dissolve the reacted dye. The absorbance of each well was read on a microplate reader (SQuant Biotek) at 540 nm. The control experimental medium contained no nanoparticles. The samples were maintained with uniform drug concentration. The spectrophotometer was calibrated to zero absorbance using culture medium without cells. The relative cell viability (%) related to control wells containing cell culture medium without nanoparticles was calculated by $[A]_{\text{test}}/[A]_{\text{control}} \times 100$, where $[A]_{\text{test}}$ is the absorbance of the test sample and $[A]_{\text{control}}$ is the absorbance of control sample.

Statistical analysis

All the experiments were conducted in triplicate. The statistical analysis of experimental data utilized the Student's *t*-test, and the results were presented as mean \pm S.D. Statistical significance was accepted at a level of $p < 0.05$.

RESULTS AND DISCUSSION

Effect of parameters on the particle size and entrapment efficiency

SEM revealed the spherical nature and a narrow size distribution of tamoxcL-ChtNPs and tamoxcF-ChtNPs that were efficiently prepared using an IG method in the presence of TPP as cross-linking agent (Figs. 1a,b). The effects of three different variables (pH, concentration of chitosan, and TPP) on the par-

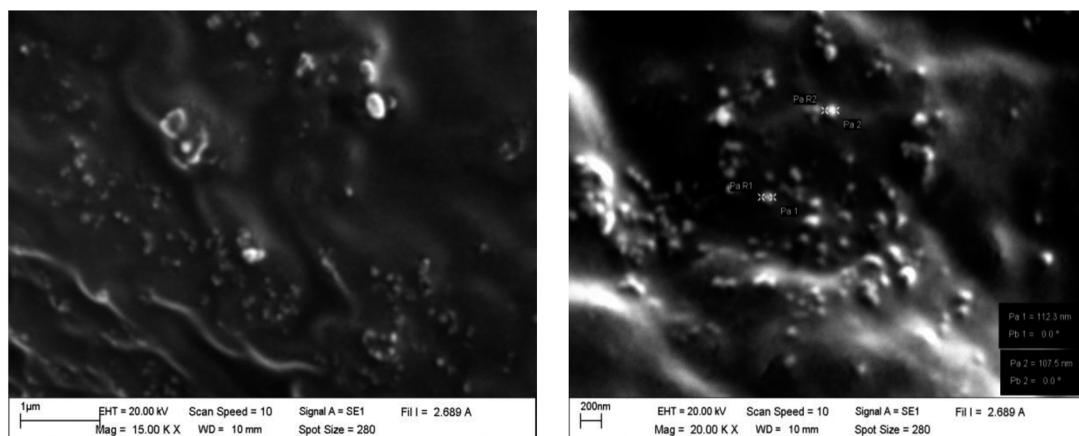


Fig. 1 SEM photomicrographs of (a) tamoxcF-ChtNPs, (b) tamoxcL-ChtNPs.

ticles size, size distribution, and drug EE of ChtNPs were studied. We prepared the nanoparticles by changing one variable and keeping other two variables constant in each experiment. The influence of pH was evident on incorporation of tamoxc into the chitosan nanoparticles. This may be due to the hydration of free-amino groups of chitosan in aqueous acetic acid ($\text{pH} \pm 3.05$). The chitosan with a $\text{p}K_a$ of 6.3 is polycation when dissolved in acid and presents free $-\text{NH}_3^+$ sites. Similarly, sodium tripolyphosphate ($\text{Na}_5\text{P}_3\text{O}_{10}$) in aqueous system dissociates to give both hydroxyl and phosphoric ions. Hence, the cross-linking of chitosan would mainly be dependent on the availability of the cationic sites on the chitosan and the anionic sites on the TPP.

The nanoparticles were much bigger at pH 2 (389 nm with PDI 0.187) in comparison to pH 4 (226 nm with PDI 0.164) and pH 5 (294 nm with PDI 0.157) of chitosan solution with chitosan (0.1 %) and TPP (0.6 %) (Fig. 2a). Surprisingly, a sudden decrease in size of the particles was noticed at pH 3 (187 nm with PDI of 0.125) that may be due to saturation of TPP binding with the available free-amino groups of chitosan. Upon adjusting the pH of TPP to 3 produced phosphoric ions to interact with the available $-\text{NH}_3^+$ groups of chitosan that resulted in the formation of smaller nanoparticles. A slightly larger particle size at higher pH was noticeable, and it may be due to the presence of both OH^- and phosphoric ions, which might compete with each other to interact with the $-\text{NH}_3^+$ of chitosan. The chitosan-TPP complex at lower pH was formed by the ionic interaction between positively charged chitosan and negatively charged phosphoric ions while at the higher pH, deprotonation of $-\text{NH}_3^+$ groups

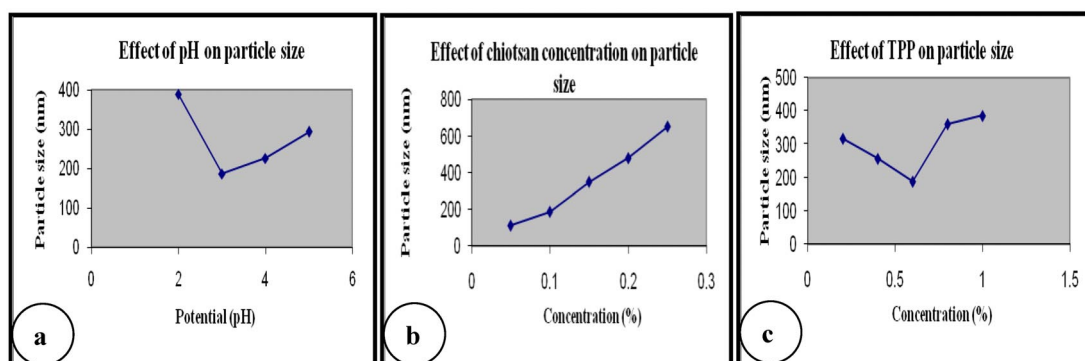


Fig. 2 Effect of pH, amount of chitosan polymer, and TPP concentration on nanoparticle size.

of chitosan was understandable. The increase in particle size at pH 4 and 5 might be due to the degree of deprotonation of amino groups of chitosan. During the process of interaction, deprotonation of free-amino groups (pK_a 6.4) had led to weaker ionic interactions between the $-\text{NH}_3^+$ groups and TPP anions. To determine the effect of chitosan concentration on size of the nanoparticles, pH and TPP (pH 3 and 0.6%) variables were kept constant and chitosan concentration was varied. Chitosan solution concentration ranging between 0.05 and 0.1 % was able to produce the smaller sized particles (112 and 187 nm) with size distributions (PDI) of 0.069 and 0.125, respectively. But, the size of the particles began to increase on increasing the concentration of chitosan solution from 0.1 to 0.25 % to yield larger particles ranging from 349 to 650 nm with PDI of 0.125 to 0.349 (Fig. 2b). The results could be attributed that increased concentration of chitosan solution in the preparation system would certainly influence on the viscosity rise. While determining the effect of TPP concentration on the size of nanoparticles, the pH 3 and chitosan concentration (0.1 %) was kept constant and the TPP concentration was only varied. An incremental rise of TPP from 0.2 to 1.0 % caused a decrease in particle size gradually until 0.6 % (317 to 187 nm) with narrow size distributions (PDI) of (0.284 to 0.125). Further, the addition of TPP influenced the size increase at 0.8 % (361 nm with 0.364 PDI) and 1.0 % (386 nm with 0.256 PDI) concentration (Fig. 2c). This increase in the particle size may be due to saturation of cationic groups ($-\text{NH}_3^+$) on chitosan solution to the incoming anionic groups ($\text{P}_3\text{O}^{5-}_{10}$) from TPP. From data, it was evident that chitosan nanoparticles could only be produced when used in a specific concentration range of chitosan and TPP. Any change in the concentration of TPP and chitosan might lead to either particle aggregation or no particle formation [23].

The DD of chitosan was calculated by titrimetric method with phosphoric acid and 0.1 M sodium hydroxide using phenolphthalein as an indicator. It was found to be 87.26 % DD responsible for increased water absorption capacity of chitosan. This rise was inversely proportional to percent deacetylation and EE as reported by others [24,25]. The chitosan nanoparticles prepared showed a good EE ranging from 34.91 to 82.14 %. There was a linear decrease in EE (82.14 % to 67.5 %) with an increase in pH of the solution (Fig. 3a). It was comparable from earlier reports that maintaining the pH of the solution at the isoelectric point would improve the EE of the particles [26,27]. The EE of tamoxcL-ChtNPs was decreased from 69.4 to 34.91 % with respect to increase in chitosan concentration. When the concentration of chitosan was fixed at 0.1 % there was a slight increase in EE of 72.4 % (Fig. 3b). The EE of tamoxc in tamoxcL-ChtNPs was increased from 63.9 to 74.23 % with respect to increase in TPP from 0.2 to 0.8 %, but further increase in TPP to 1 % decreased the EE to 69.41 %. This decrease in EE at 1 % of TPP may be attributed to the saturation of the polymer matrix with the TPP, which helps form the particles (Fig. 3c).

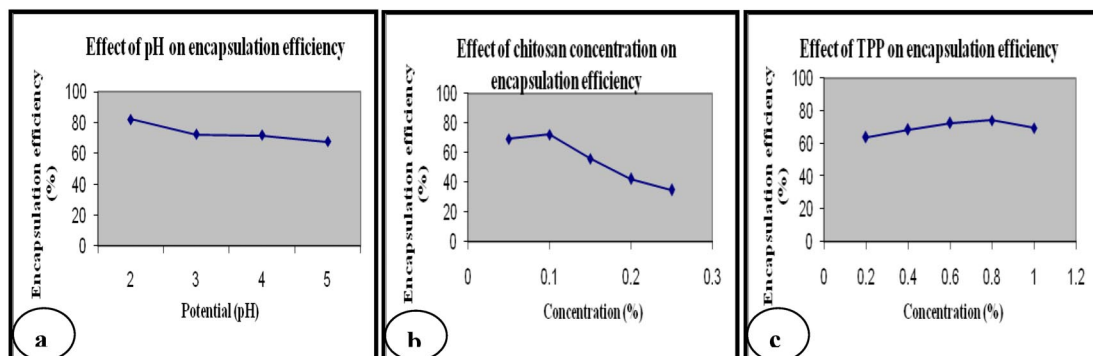


Fig. 3 Effect of pH, amount of chitosan polymer, and TPP concentration on EE of tamoxcL-ChtNPs.

ζ -potential is an index to the stability of the nanoparticles. In most cases, the higher the value of ζ -potential the larger the amount of charge on their surface, which leads to strong repulsive interaction among the nanoparticles, thus resulting in higher stability and more uniform size of the nanoparticles. In the present study, positive ζ -potential is exhibited by both tamoxcF-ChtNPs and tamoxcL-ChtNPs ranging between +9 to +30 mV. The ζ -potential of the tamoxcF-ChtNPs and tamoxcL-ChtNPs is summarized in Table 1. Among the formulations observed, the tamoxcL-ChtNPs possessed higher ζ -potential than the tamoxcF-ChtNPs, this could be accounted for deposition of the tamoxc on the surface of the particles. This difference in potential of the formulations may be due to decreased $-\text{NH}_3^+$ groups leads to decrease ζ -potential and absorption phenomenon of anionic molecules of the acidic system. In the same way, increased potential is mostly due to the increased $-\text{NH}_3^+$ groups and drug adsorptions on the surface of the nanoparticles.

Table 1 Influence of pH on the ζ -potential (ZP) of chitosan nanoparticles.

pH	Formulations	ZP (mV)
pH 2	TamoxcF-ChtNPs	+13.4
	TamoxcL-ChtNPs	+9
pH 3	TamoxcF-ChtNPs	+20.2
	TamoxcL-ChtNPs	+19.1
pH 4	TamoxcF-ChtNPs	+25.4
	TamoxcL-ChtNPs	+23.8
pH 5	TamoxcF-ChtNPs	+30
	TamoxcL-ChtNPs	+28.6

Fourier transform infrared spectroscopy (FTIR) analysis

FTIR spectra of (a) chitosan polymer alone, (b) tamoxc, (c) tamoxcF-ChtNPs, and (d) tamoxcL-ChtNPs have been shown in Figs. 4a–d. The three characterization peaks at 3436 cm^{-1} ($-\text{OH}$), 1575 cm^{-1} ($\text{C}-\text{O}-\text{C}$) and 1091 cm^{-1} ($-\text{NH}$) were taken into account. Among two varieties of nanoparticles, the spectrum of tamoxcL-ChtNPs looked different from that of tamoxcF-ChtNPs. In comparison, the peak 3436 cm^{-1} of tamoxcF-ChtNPs was much wider than tamoxcL-ChtNPs, indicating stretching of hydrogen bonds (Figs. 4c,d). A peak at 1596 cm^{-1} noticed in tamoxcF-ChtNPs was found to be shifted in tamoxcL-ChtNPs along with a peak at 2932 cm^{-1} of the drug tamoxc. From the dissolution point of view, the solvation of chitosan is related to the protonation of free amine groups and breakdown of strong intra- and intermolecular hydrogen bonding. The H-bonding established through $-\text{NH}_2$ linkage makes the molecule behave as a resonating structure owing to unshared electron pairs that are less available for protonation. In addition, nitro groups withdraw electrons, making them less accessible at the secondary amide and primary amide groups during interaction. It is evident from the graph that there is a possible interaction between tamoxc and chitosan. A shift in the peak of tamoxcL-ChtNPs indicates the interaction of chitosan with tamoxifen. The change indicates encapsulation of tamoxifen to form ChtNPs successfully. Since the surface of tamoxifen (with little negative charges) has an affinity toward chitosan, polycation chitosan could bind tamoxifen by the electrostatic interaction and chemical reaction.

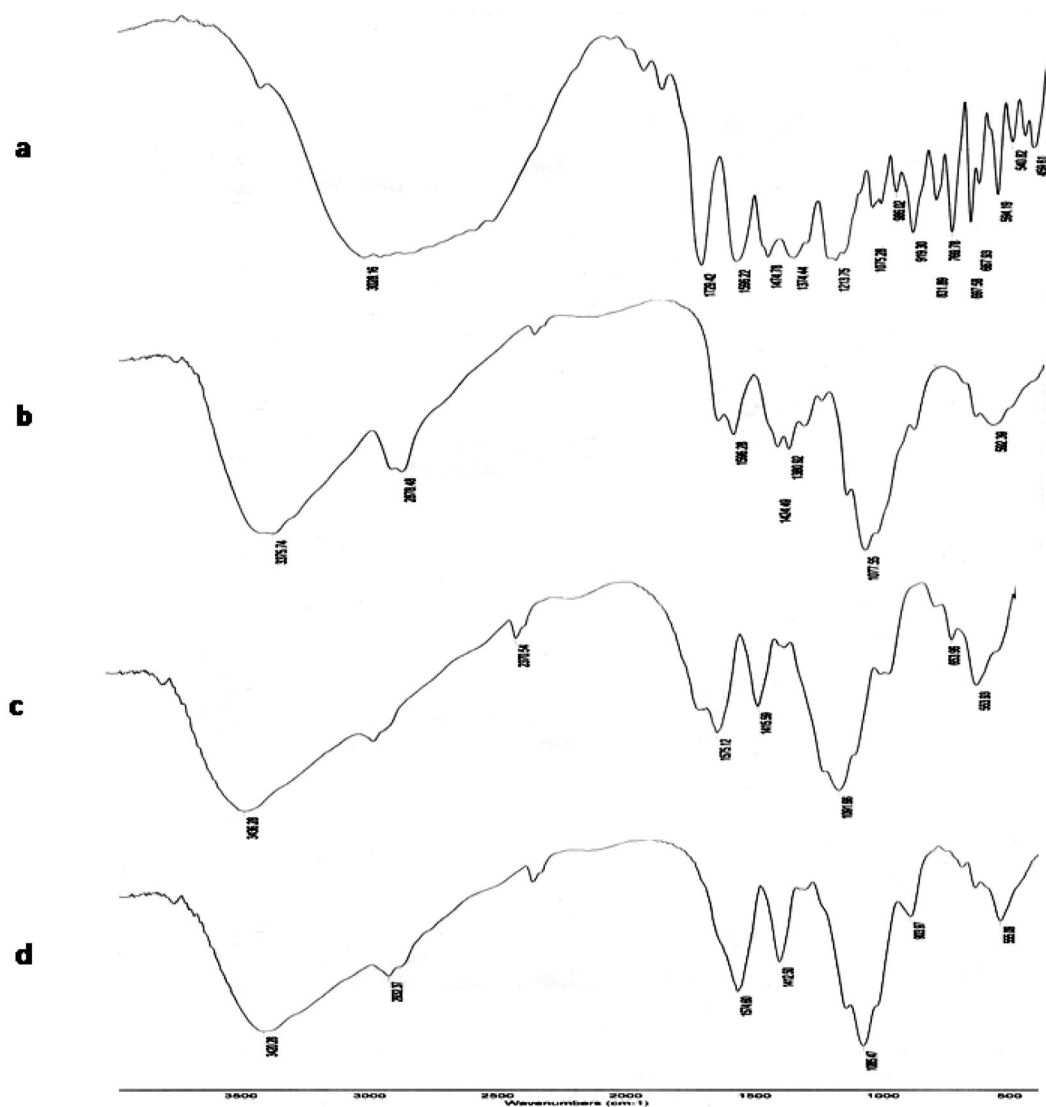


Fig. 4 FTIR spectra of (a) chitosan polymer alone, (b) tamoxc and (c) tamoxcF-ChtNPs, and (d) tamoxcL-ChtNPs.

Differential scanning calorimetry (DSC)

DSC studies were conducted using Mettler-Toledo DSC. The thermogram of tamoxcF-ChtNPs showed endotherm at 154.2 °C with enthalpy of fusion 377.8 J/g and exothermic peak at 280.0 °C (Fig. 5a). The thermal event observed at 280.0 °C was due to the decomposition of the polymer. It was different in the case of tamoxcL-ChtNPs where the thermogram at 164.5 °C exhibited an endothermic change with a slightly wider peak showing onset and endset trends at 140.7 °C and 184.6 °C, respectively (Fig. 5b). Interestingly, a characteristic endothermic peak at 146.1 °C was noticeable with enthalpy change by 392.6 J/g. This corresponded to the peak of tamoxc at 146.1 °C with enthalpy of fusion at 103.4 J/g (Fig. 5c) used as reference. The results may be attributed to cross-linking of chitosan with TPP modifying the crystalline nature of tamoxc. From Figs. 5a–c, polymorph change of the drug or drug polymer

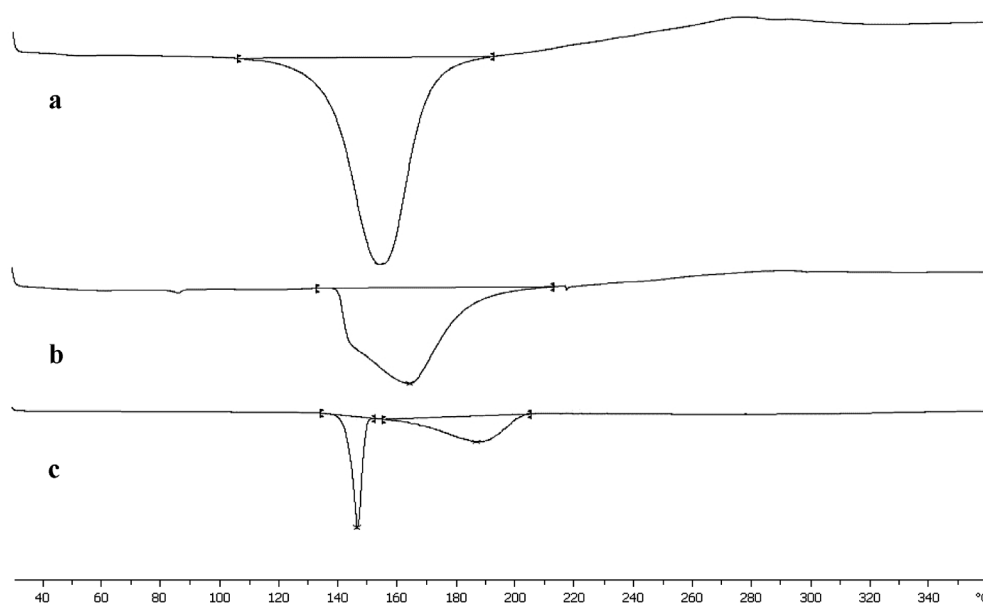


Fig. 5 DSC thermographs of (a) tamoxc, (b) tamoxcF-ChtNPs, and (c) tamoxcL-ChtNPs.

interactions (e.g., plasticizing effect of drug on polymer) can be observed as peak shifts in the DSC thermogram.

From data, a shift in the peak can be observed in the tamoxcL-ChtNPs as it shows the peak at 146.19 °C with an additional peak at 187.56 °C. This may be due to interaction of the tamoxc with chitosan. The observations made by other researchers have also emphasized similar results assumed to be due to increase in the polar groups. As crystalline domains of chitosan nanoparticles exhibit cross-linking, it enhances the H-bonding leading to hold more water. Hence, the water-holding capacity of any given polymer would be different from its cross-linked polymer at set conditions [28].

Drug release studies

Drug release studies were carried out at physiological pH 7.4, and the profile of tamoxc release from tamoxcL-ChtNPs (Fig. 6) was compared with the free-tamoxc as reference standard. When compared to the release of tamoxc from tamoxcL-ChtNPs, the release was much slower than the release of free-tamoxc from the dialysis bag in 6 h. The release of encapsulated tamoxc from tamoxcL-ChtNPs was an initial burst of more than 35 % from the dialysis bag, it established just in an hour. In fact, about 35.94 % (~0.90 mg) drug release was observed in the first 12 h, later the release of drug was comparatively much slower, which continued to release until 48 h. The delay in release of tamoxc from tamoxcL-ChtNPs was much slower in the later phase and took nearly 48 h in order to get release 47.34 % (~1.19 mg) out of 2.5 mg of the drug in the formulation. This kind of rapid release followed by slow and sustained release of tamoxc appears to be indicative of biphasic release pattern of the tamoxcL-ChtNPs. This may be because of the tamoxc that was embedded in the chitosan matrix of nanoparticles, which might have taken a little extra time to get released from the encapsulating polymer (Fig. 6). The difference in release from the dialysis bag for both free tamoxc and loaded tamoxc is evidently attributed to the prolonged release function of the nanoparticle [29]. This means that tamoxc in tamoxcL-ChtNPs can be released slowly and kept at a constant concentration for a long period both in vitro and in vivo, which is very important for the clinical application.

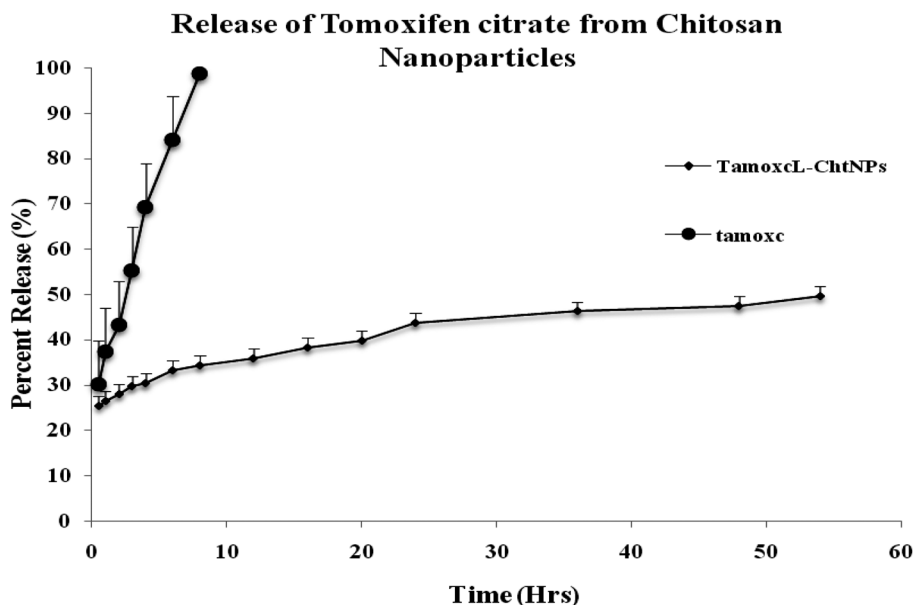


Fig. 6 Release of tamoxc from tamoxcL-ChtNPs.

Blood compatibility

Hemolysis study was conducted to ascertain the safety of the nanoparticles prepared using human RBCs. In the assay, the samples (except water) were taken in three different concentrations 1.5, 3, and 5 mg to compare the degree of damage to RBCs in comparison with distilled water. The hemolysis of RBCs was within the permissible range of about 0.6 to 1.02 % for tamoxcF-ChtNPs, whereas a slightly increased trend was noticed in the case of tamoxcL-ChtNPs, showing 7.3 to 13.2 % hemolysis. But the hemolysis was still higher in the free drug tamoxc, showing 18.3 to 22.01 %. From data, it was understandable that as the concentration of drug in tamoxcL-ChtNPs was much lower in comparison to tamoxc, it exhibited lower adverse effect than the latter. According to researchers, about 5 % hemolysis may not cause much adverse effect to the system and may be accepted as within permissible limit [30,31]. Very insignificant adverse effect was observed in the case of tamoxcF-ChtNPs ($P < 0.05$). In comparison, the damage assessed was rather more by tamoxc than tamoxcL-ChtNPs, which exhibited nearly 40 % less damage (Fig. 7) ($P < 0.05$). It has been specified that hemolysis caused by chitosan less than 15 % would be welcomed and considered as not hemolytic [32].

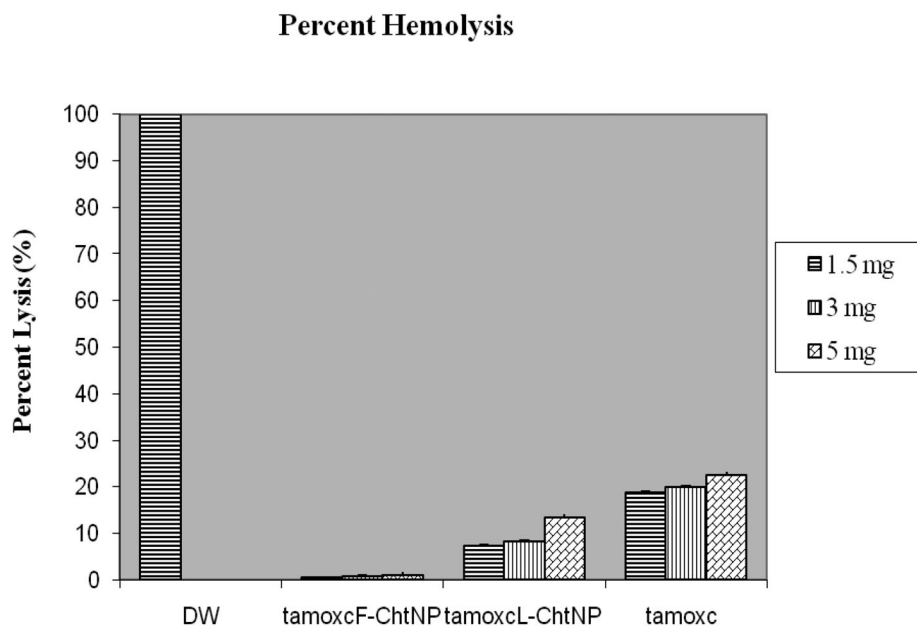


Fig. 7 Determination of relative hemolysis in the presence of (a) distilled water, DW (b) tamoxcF-ChtNPs, (c) tamoxcL-ChtNPs, and (d) tamoxc, at three different concentrations.

In vitro cytotoxic assay

The proliferation/viability of cells was measured by MTT assay after culturing for 48 h. The cytotoxicity of tamoxc on MCF-7 and Vero cells is shown in Figs. 8a,b, respectively. The cytotoxic effects of nanoparticles increased with an increase in tamoxc concentration. The toxicity of tamoxc was increased as the concentration raised from 1 to 50 μM . The toxic effect of tamoxc markedly decreased the cells viability from 87.52 to 18.99 % (for MCF-7) and 94.23 to 22.41 % (for Vero cells). But the toxic effect of tamoxcL-ChtNPs showed superiority in decreasing the viability of cells from 91.33 to 4.05 % (for MCF-7) and 91.82 to 7.92 % (for Vero cells). In this cytotoxicity test, tamoxcL-ChtNPs caused a little more death of viable cells than tamoxc (free drug). In turn, tamoxcF-ChtNPs (blank nanoparticles) failed to produce any toxicity to viable cells and exhibited viability of 103.81 % (for MCF-7) and 98.67 % (for Vero cells). It was noticeable that the difference in cell viability among the MCF-7 and Vero cells for tamoxc and tamoxcL-ChtNPs was highly significant ($P < 0.05$). More interestingly, tamoxc and tamoxcL-ChtNPs exhibited toxicity at a level of $p < 0.05$ in comparison to control. This increased toxicity may be due to preferential uptake of nanoparticles (tamoxcL-ChtNPs) than that of free drug (tamoxc).

The results showed that the cytotoxicity of tamoxcL-ChtNPs was nearly the same as that of tamoxc and in comparable with previous studies [33,34,29]. The possible mechanism underlying the slightly enhanced efficacy of tamoxcL-ChtNPs against MCF-7 and Vero cells may include the enhanced intracellular drug accumulation by nanoparticle uptake. Previous reports supported the current findings by determining the cytotoxicity of tamoxcL-ChtNPs at different concentrations [35,36]. As shown in Figs. 8a and b, tamoxcL-ChtNPs showed significant increase in cell death than tamoxc alone. From experimental evidence, the mechanisms underlying the superiority of toxicity shown by tamoxcL-ChtNPs against tamoxc may include the continuous exposure of viable cells to released tamoxc from the nanoparticles. Therefore, the sustained release of tamoxc was capable of exhibiting its cytotoxic efficiency constantly. It has been reported that cytotoxic activity and tumor-shrinking properties of chemotherapeutics depend on the dose and exposure time [37].

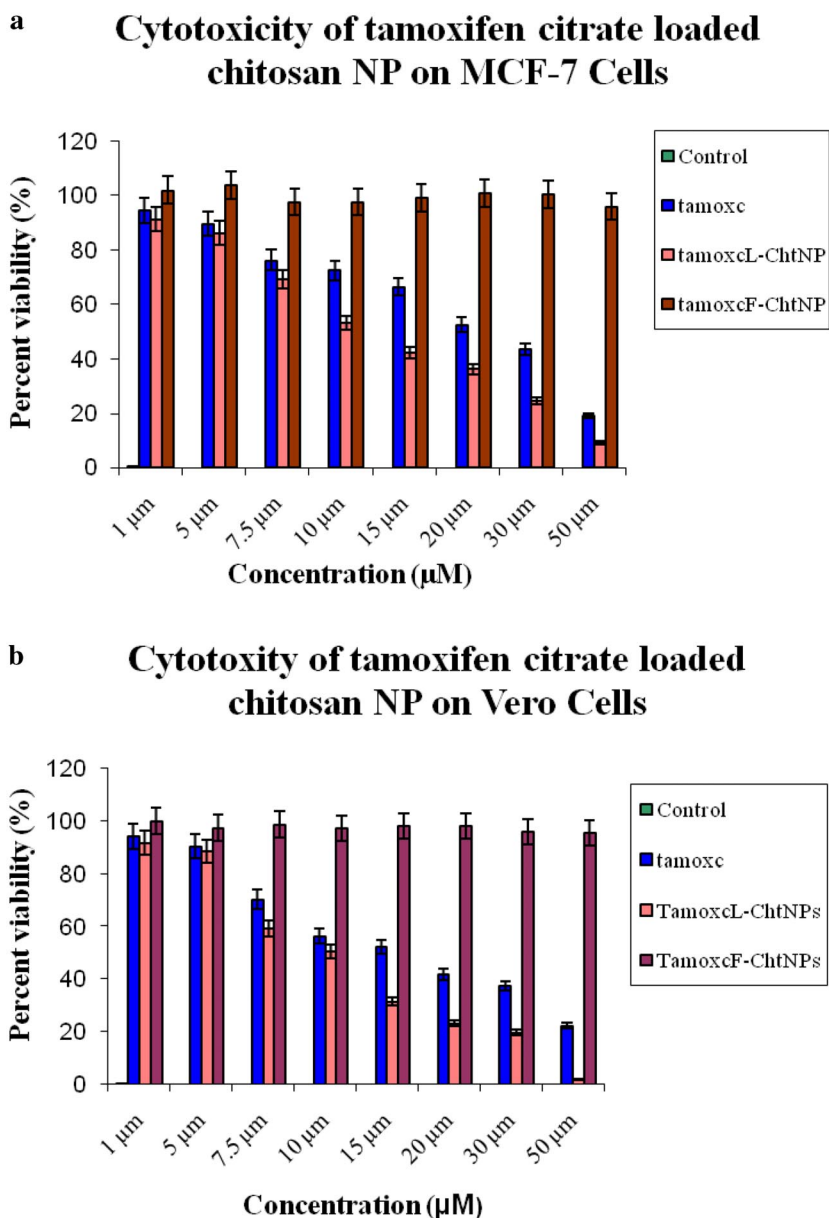


Fig. 8 Cytotoxicity of tamoxc, tamoxcL-ChtNPs, tamoxcF-ChtNPs on (a) MCF-7 cells at 48 h, (b) Vero cells at 48 h.

CONCLUSIONS

In this study, tamoxcF-ChtNPs and tamoxcL-ChtNPs were prepared using an IG method under laboratory conditions using TPP as cross-linker and characterized for their drug delivery applications. After the preparation of drug-loaded nanoparticles, conditions were optimized to obtain stable, small, and uniformly distributed chitosan nanoparticles for better encapsulation and release characteristics. TamoxcL-ChtNPs showed high EE owing to the lipophilicity of tamoxc. The in vitro release study revealed a sustained and continuous release pattern of tamoxcL-ChtNPs at physiological pH. They

exhibited reduced hemolytic activity to make them fit for pharmacological applications. The nanoparticles were nontoxic to cells even at high concentration of nanoparticles. The *in vitro* studies proved the cytotoxicity of tamoxifen-CHT-NPs in a dose- and time-dependent manner against MCF-7 and Vero cells. The results of this study are very encouraging for the development of chitosan nanoparticles as an intracellular delivery system for drugs. Because of their MCF-7 and Vero cells targeting capabilities, investigations with chitosan nanoparticles for receptor-mediated endocytosis would be advantageous. Further, employing nanoparticles of chemotherapeutics in targeted drug delivery applications suggests a special focus on reduction in side-effects as well as dosing frequency to one and merits further evaluation using an appropriate animal model for patient's compliance is warranted.

ACKNOWLEDGMENTS

The authors thank Dr. Lakshmisha, I. P., Central Institute of Fisheries Technology, Cochin, India, for the kind gift of chitosan and input in preparation; Dr. T. S. Nagaraj (SJM Pharmacy College, Chitradurga, Karnataka, India) for help with protocol and valuable input in sample preparation; and Mr. Yogananda (Department of Pharmaceutics, SJM Pharmacy College, Chitradurga, Karnataka, India) for help in release kinetics modeling. RNR gratefully acknowledges Mr. Amit J. Thakkar, Managing Director, Union Park Chemicals (Bombay) Ltd., Mumbai, India for partial financial support. The authors are thankful to Kuvempu University and Davanagere University for providing laboratory facilities and constant encouragement during this study.

REFERENCES

1. J. I. MacGregor, V. C. Jordan. *Pharmacol. Res.* **50**, 151 (1998).
2. R. M. O'Regan, V. C. Jordan. *Lancet Oncol.* **3**, 207 (2002).
3. S. G. Pappas, V. C. Jordan. *Cancer Metastasis Rev.* **21**, 311 (2002).
4. T. J. Powles. *Eur. J. Cancer.* **39**, 572 (2003).
5. C. Peters-Engl, W. Frank, E. Danmayr, H. P. Friedl, S. Leodolter, M. Medl. *Breast Cancer Res. Treat.* **54**, 255 (1999).
6. I. Cohen. *Gynecol. Oncol.* **94**, 256 (2004).
7. G. R. de Lima, G. Facina, J. Y. Shida, M. B. C. Chein, P. Tanaka, R. C. Dardes, V. C. Jordan, L. H. Gebrim. *Eur. J. Cancer* **39**, 891 (2003).
8. J. S. Chawla, M. M. Amiji. *Int. J. Pharm.* **249**, 127 (2002).
9. Y. H. Bae, K. M. Huh, Y. Kim, K. Park. *J. Controlled Release* **64**, 3 (2000).
10. H. Ge, Y. Hu, X. Jiang, D. Cheng, Y. Yuan, H. Bi, C. Yang. *J. Pharm. Sci.* **91**, 1463 (2002).
11. M. N. V. Ravi Kumar. *React. Funct. Polym.* **46**, 1 (2000).
12. K. T. Hwang, S. T. Jung, G. D. Lee, M. S. Chinnan, Y. S. Park, H. J. Park. *J. Agric. Food Chem.* **50**, 1876 (2002).
13. P. Calvo, C. Remunan-Lopez, J. L. Vila-Jato, M. J. Alonso. *J. Appl. Polym. Sci.* **63**, 125 (1998).
14. M. Prabakaran, J. F. Mano. *Drug Deliv.* **12**, 41 (2005).
15. H. D. Soule, J. Vazquez, A. Long, S. Albert, M. Brennan. *J. Natl. Cancer Inst.* **51**, 1409 (1973).
16. A. S. Levenson, V. C. Jordan. *Cancer Res.* **57**, 3071 (1997).
17. N. O. Bianchi, J. Ayres. *Exp. Cell Res.* **68**, 253 (1971).
18. V. R. Haas, A. R. Santos Jr., M. L. F. Wada. *Cytobios.* **106**, 255 (2001).
19. J. Knapczyk, L. Krowczynski, J. Krzek, M. Brzeski, E. Nurnberg, D. Schenk, H. Struszczyk, G. S. Braek, T. P. Anthonsen, P. A. Sandford. "Requirements of chitosan for pharmaceutical and biomedical application", in *Chitin and Chitosan: Sources, Chemistry, Biochemistry, Physical Properties and Applications*, pp. 657–663, Elsevier Science, New York (1989).
20. P. Calvo, C. Remuñan-López, J. L. Vila-Jato, M. J. Alonso. *Pharm. Res.* **14**, 1431 (1997).

21. N. R. Ravikumara, T. S. Nagaraj, R. Hiremat Shobharani, G. Raina, B. Madhusudhan. *J. Biomater. Appl.* **24**, 47 (2009).
22. T. Mosmann. *J. Immunol. Methods* **95**, 55 (1993).
23. G. Liu, L. Shao, F. Ge, J. Chen. *China Particuology* **5**, 384 (2007).
24. I. Bravo-Osuna, G. Millotti, C. Vauthier, G. Ponchel. *Int. J. Pharm.* **338**, 284 (2007).
25. D. R. Bhumkar, V. B. Pokharkar. *AAPS Pharm. Sci. Tech.* **7**, E1 (2006).
26. Y. Xu, Y. Du. *Int. J. Pharm.* **250**, 215 (2003).
27. F. S. Kittur, K. V. Harish Prashanth, K. Udaya Sankar, R. N. Tharanathan. *Carbohydr. Polym.* **49**, 185 (2002).
28. J. Autian, R. L. Kronenthal, Z. Oser, E. Martin (Eds.). "Biodegradable polymers in medicine and surgery", in *Polymers in Medicine and Surgery*, pp. 181–203, Plenum Press, New York (1975).
29. X. Li, R. Li, X. Qian, Y. Ding, Y. Tu, R. Guo, Y. Hu. *Eur. J. Pharm. Biopharm.* **70**, 726 (2008).
30. R. K. Dey, A. R. Ray. *Biomaterials* **24**, 2985 (2003).
31. R. K. Dey, A. R. Ray. *J. Appl. Polym. Sci.* **90**, 4068 (2003).
32. S. C. W. Richardson, H. V. J. Kolbe, R. Duncan. *Int. J. Pharm.* **178**, 231 (1999).
33. L. Zhang, Y. Hu, X. Jiang, C. Yang, W. Lu, Y. Yang. *J. Controlled Release* **119**, 153 (2007).
34. L. Zhang, Y. Hu, X. Jiang, C. Yang, W. Lu, Y. Yang. *J. Controlled Release* **96**, 135 (2004).
35. D. Le Garrec, S. Gori, L. Luo, D. Lessard, D. C. Smith, M. A. Yessine, M. Ranger. *J. Controlled Release* **99**, 83 (2004).
36. E. van Vlerken, Z. Duan, M. V. Seiden, M. M. Amiji. *Cancer Res.* **67**, 4843 (2007).
37. T. S. Bekaii-Saab, M. A. Villalona-Calero. *Semin. Oncol.* **32**, S3 (2005).